

Collaborative Attention Network for Person Re-identification

Wenpeng Li¹, Yongli Sun¹, Jinjun Wang^{2, 1*}, Han Xu¹, Xiangru Yang¹, Long Cui¹
¹Deep North Inc., ²Xian Jiao Tong University

¹{wpli, ylsun, hxu, xryang, lcui}@deepnorth.cn, ²jinjun@mail.xjtu.edu.cn

Abstract

Jointly utilizing global and local features to improve model accuracy is becoming a popular approach for the person re-identification (ReID) problem, because previous works using global features alone have very limited capacity at extracting discriminative local patterns in the obtained feature representation. Existing works that attempt to collect local patterns either explicitly slice the global feature into several local pieces in a handcrafted way, or apply the attention mechanism to implicitly infer the importance of different local regions. In this paper, we show that by explicitly learning the importance of small local parts and part combinations, we can further improve the final feature representation for Re-ID. Specifically, we first separate the global feature into multiple local slices at different scale with a proposed multi-branch structure. Then we introduce the Collaborative Attention Network (CAN) to automatically learn the combination of features from adjacent slices. In this way, the combination keeps the intrinsic relation between adjacent features across local regions and scales, without losing information by partitioning the global features. Experiment results on several widely-used public datasets including Market-1501 [31], DukeMTMC-ReID [12] and CUHK03 [21] prove that the proposed method outperforms many existing state-of-the-art methods.

1. Introduction

The person re-identification (Re-ID) problem is one of the most significant yet challenging tasks in the computer vision area. The input data for person Re-ID system are mostly the full body bounding boxes of pedestrian detected from multiple surveillance cameras. The person Re-ID task then helps to retrieve a certain person among all the bounding box images by figuring out under which cameras the person appears and re-appears. Comparing with a typical face recognition system where facial images are usu-



Figure 1. These four pairs of bounding box images are from Market-1501 dataset [31], and each pair shows slight difference between two persons. Global feature models are not sufficient to identify one person from another.

ally obtained from a constrained environment, person Re-ID is more applicable in real-world scenario where factors such as occlusion, posture change and illumination variation among different cameras further complicate this problem.

In recent years, deep neural networks have been proven effective at extracting discriminative features for the images classification problem [2, 5, 7], and are therefore widely used as the base model of person Re-ID approaches. For instance, previous works [3, 11] proposed standard baselines in which ResNet [5] was used to extract the appearance feature of the full body image. Since such network model obtains only a global representation, model performance is limited at distinguishing bounding box images with minor difference. The baseline methods based on [5] only obtains a global feature such as the overall color of clothing which is insufficient for person Re-ID. Some examples are shown in Figure 1. Global features for persons with similar clothing are close to each other in feature space, which makes it hard for baseline models to distinguish different person IDs from each other for each pair. We typically identify persons

*Corresponding author, jinjun@mail.xjtu.edu.cn

not only by general clothing colors but also by local details which cannot be obtained by global feature representations. To improve the performance of such base model that extract only the global feature, local features are also attempted by attaching to the original global features for more discriminative representation capacity. For example, [13] addressed the issue by collecting representative patches from the image, and the trained model show good balance between discriminative power and generalization ability. For a more explicit part-based feature representation for Re-ID, [26, 29] utilized firstly a part detector to locate body parts and then extracted features from different local parts. Although experimental results validate that combining global and local features can improve the model accuracy, the definition of what parts to locate is rather arbitrary and may change dataset by dataset and/or object class by class.

To achieve a more data-driven way, researchers have also investigated the attention mechanism to implicitly infer the importance of different local regions. For example, in [1] the author proposed the High-Order Attention module that contains high-order statistics of convolutional activations. At the same time, since the part-based methods can also be viewed as learning the attention among parts, end-to-end method based on learning the importance of parts or part combinations have also been reported. To give an example, [19] proposed a part-based Re-ID models where mid-level features were divided into slices with fixed spatial location and size. Local features from these slices were then arbitrarily fused to derive the final representation. The method can be viewed as a hard combination mechanism with identical attention for each part, and leads to state-of-the-art performance. On the other hand, since the global level information will be lost when global feature is separated into too many slices, defining the proper parts or part combinations becomes challenging and may easily overfit. Our experiments on *number of parts* hyperparameter show that model accuracy will descend when increasing the granularity of slicing feature maps.

In this paper, we propose the Collaborative Attention Network to further improve over existing part-based Re-ID feature models. The idea is to automatically learn the combination of features from adjacent slices to keep the intrinsic relation between adjacent features across local regions and scales, without losing information by partitioning the global features, while generating more discriminative features based on local patterns. The contributions of this paper are two-fold:

- (i) Local features can refer the relative information from adjacent local features by introducing the Collaborative Attention Network, which makes the part-based more effective.
- (ii) We replace the FC Layer with Cosine Layer and then

use the Cosine Distance to measure feature distance and similarity, which makes our model more accurate on benchmarks.

2. Related Works

With the massive development of deep learning and neural networks, person Re-ID methods have made great progress from traditional hand-craft feature extraction to deep-learned neural network models. Release of public person Re-ID dataset [31, 12, 21, 22], researchers can train Re-ID models over a large scale of image data. Specifically for person Re-ID topic, some metric learning methods were proposed, which can properly discipline the training process. Partial features are proven to be useful because of the particularity of person retrieval problem, since persons are distinguished between each other by local details.

2.1. Part-based Methods for Person Re-ID

The major contribution of this paper is a more effective part-based model. We compare our proposed model with existing part-based methods which are useful when learning feature representation for person Re-ID. Some methods used body segmentation network or landmark detectors [15, 26, 8] as prerequisite of part-based model and achieved great progress. However, since datasets for training such detectors are different with person retrieval datasets, these methods do not perform perfectly. In [19], the author proposed the Part-Based Convolutional Baseline (PCB) in which a uniform partition on global features was used. Then these local features were used for classification and this method was verified to be effective yet not to be improved. Along with PCB model in this paper, the author introduced a refined part pooling (RPP) method. RPP method is the attention mechanism that can re-assign parts by image blocks instead of uniformly slicing the images. Inspired by this part-based method, recent work [20] put forward the novel Multiple Granularity Network (MGN) which is the state-of-the-art method on person Re-ID benchmarks. MGN is based on a multi-branch structure where global features and local features are combined together as the final feature representation. In branches of local features, images are separated into 2 and 3 stripes from original feature maps. By diversity of granularity, different branches are varied in feature extraction preference. Combining global features with multi-granularity local features, the feature extractor is more comprehensive. Our method in this paper is inspired by the multi-branch structure but with finer feature partition and with a more effective collaborative attention method.

2.2. Metric Learning

When doing person retrieval, we need to identify or classify certain persons among all detected pedestrians. In public datasets, each person is assigned with a unique person

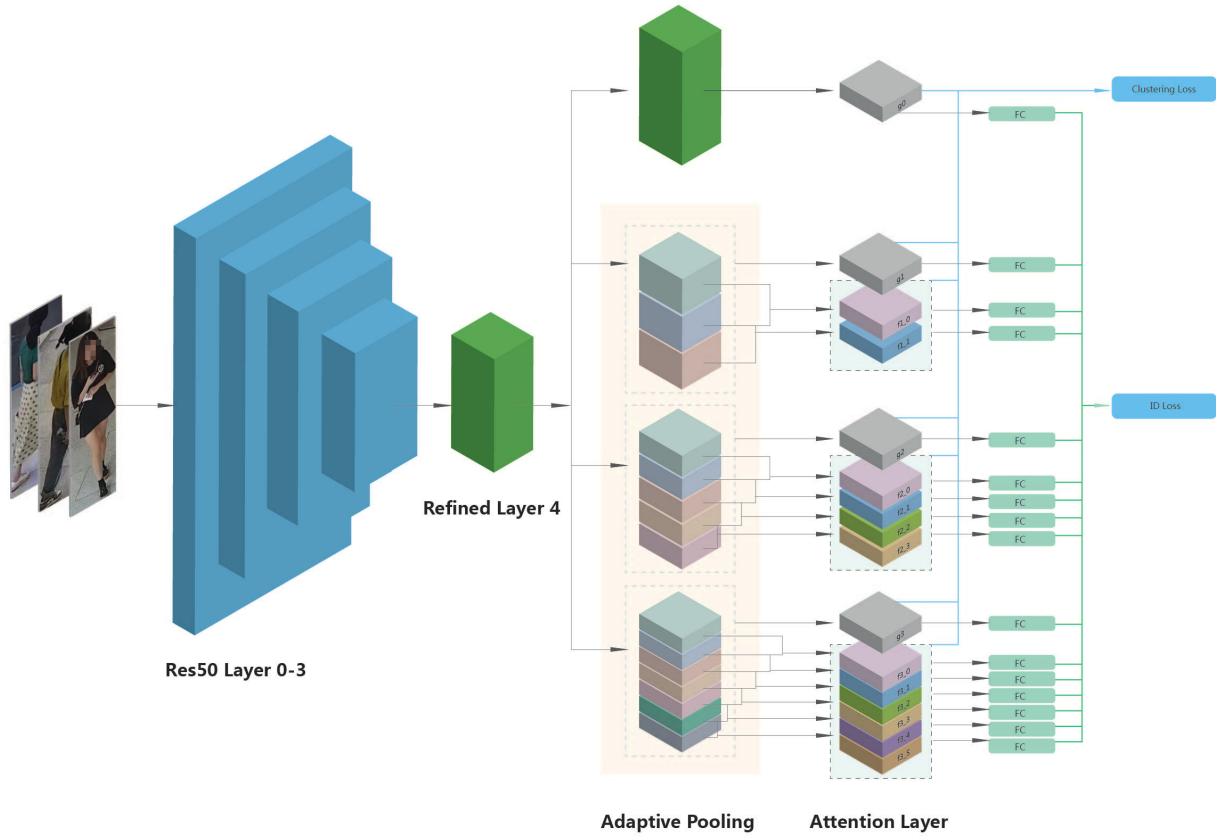


Figure 2. Pipeline of our proposed Collaborative Attention Network (CAN). ResNet50 is used as base model but we refine the Layer 4 in ResNet50 to give out more detailed features. Collaborative Attention method is introduced for partial feature branches. A multi-loss function is employed to make the feature representation more discriminative.

ID which makes person re-identification is essentially similar to classification problem. ID loss such as Cross Entropy is necessary for classification model training. However, in order to achieve discriminative features, metric learning with multiple loss functions becomes a widely-used strategy. Besides ID loss, loss functions to measure the feature similarities are introduced during training process. Triplet Loss [6] is firstly used for person Re-ID by setting the training batches with several person IDs. Identical and different IDs are respectively viewed as positive and negative samples in Triplet Loss. To step further, SphereReID [25] was proposed in which the feature vectors were mapped into hypersphere manifold and distances on the new feature space were calculated to measure feature similarity instead of using the Euclidean Distance. With these loss function, metric learning can properly guide the training process and the learned features are more discriminative.

3. Method

3.1. Overview

Figure 2 shows the network architecture of our Collaborative Attention Network (CAN). CAN is a multi-branch network in which local branches and global branches separately generate features vectors and we concatenate all these features to give out the final feature vector. Collaborative Attention module and the design of multi-loss function are two significant factors in our proposed method.

3.2. Network Structure

ResNet50 is utilized as base model in our network. Instead of using the entire feature extractor, we only use *Layer0* to *Layer3* in base model. In order to keep more details in feature maps, we refine *Layer4* of ResNet50 which outputs $2048 \times 24 \times 8$ features maps, where 2048 is the feature dimension and 24×8 is the feature size. After the

refined *Layer4*, the model is separated into four branches with the feature size for each branch. In different local feature branches, we slice feature maps uniformly into different number of parts. Therefore, we employ Adaptive Pooling for each branch. The advantage of Adaptive Pooling is that it can adaptively adjust the pooling kernel by the given input and output size. For the normal pooling, given the *kernel_size*, *padding*, *stride* and the size of input tensors *input_size*, then the *output_size* can be formulated as:

$$output_size = \frac{(input_size + 2 * padding - kernel_size)}{stride} + 1 \quad (1)$$

From Equation 2, we can infer the *kernel_size* given the other parameters:

$$kernel_size = (input_size + 2 * padding) - (output_size - 1) * stride \quad (2)$$

As a result, the *padding*, *stride* and *kernel_size* for Adaptive Pooling can be defined as:

$$\begin{cases} padding = 0 \\ stride = \mathbf{floor}(input_size/output_size) \\ kernel_size = input_size \\ \quad - (output_size - 1) * stride \end{cases} \quad (3)$$

In order to enrich the information from feature maps, we expand feature dimensions by concatenating max and average pooling output. After the Adaptive Pooling Layer in the network structure, the feature dimension for each branch is shown in Table 1

Branch	Feature map size	Feature dimension
global	1*1	2048*2
part-3	3*1	2048*2
part-5	5*1	2048*2
part-7	7*1	2048*2

Table 1. Sizes and dimensions after Adaptive Pooling.

After achieving a hierarchical structure by specifying various output sizes for Adaptive Pooling, the feature maps are fed into the Collaborative Attention Layer. The Collaborative Attention module is shown in Figure 3. This module is applied in each local feature branch and the experimental results show that this module can give out a better performance comparing with existing part-based methods. We argue that for different scales of local features, the global features learning by the neural network could be varied.

For each local feature branch, before we partition the feature map into stripes, an auxiliary global feature branch is pulled out by apply Adaptive Pooling. Unlike other existing part-based method, we collaboratively combine two adjacent local features $\{P_{i,k}, P_{i,(k+1)}\}$ from *part_i* branch, in which $k \in \{0, 1, \dots, (i-2)\}$. Each collaborative feature is 4096-dimensional with size $2 * 1$ and feature set after the max pooling is $Fa = \{fa_{i,0}, fa_{i,1}, \dots, fa_{i,(n-1)}\}$ where $n = i - 1$ for *part_i* branch. Since each feature in this feature set is 4096-dimensional, it will be excessively redundant when the local features are concatenated to form the final feature. To fix this problem, a $1 * 1$ convolutional layer is employed. On one hand, $1 * 1$ convolution can be used to reduce feature dimensions. However, in our consideration, the weights in convolutional layer can act as channel attention values while the collaborative concatenation is a hard spatial attention method. The channel attention weights set is $W^T = \{w_1^T, w_2^T, \dots, w_m^T\}$ where $m = 256$ is the final feature dimension for each branch. Then the Attention Layer can be expressed by Equation 4:

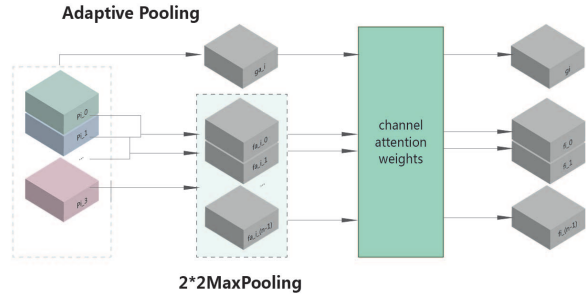


Figure 3. Collaborative Attention module.

$$W^T F a = \{f_{i,0}, \dots, f_{i,(n-1)}\} = \{W^T fa_{i,0}, \dots, W^T fa_{i,(n-1)}\} \quad (4)$$

For each local branch, the feature vector is $f_{i,k}$ where $k \in \{0, 1, \dots, (n-1)\}$ and it can be formulated as:

$$f_{i,k} = W^T fa_{i,k} = \{w_1^T fa_{i,k}, w_2^T fa_{i,k}, \dots, w_m^T fa_{i,k}\} = [f_{i,k_0}, f_{i,k_1}, \dots, f_{i,k_{m-1}}] \quad (5)$$

After processed by our proposed Collaborative Attention Network, we obtain four 256-dimensional global feature maps and twelve 256-dimensional local features maps.

3.3. Loss Function and Metric Learning

The design of loss function is crucial when training the models. Typical strategy of loss function for person ReID

task is to combine ID loss and Triplet Loss. ID loss can supervise the model to perform when doing for person classification and Triplet Loss make the model discriminate in-apparent feature difference. Along with ID loss and Triplet Loss, center loss [11, 24] is also applied in our loss function. The overall loss function can be formulated as:

$$\mathcal{L} = \mathcal{L}_{CE} + \mathcal{L}_{Triplet} + \lambda \mathcal{L}_C \quad (6)$$

In this multi-loss function, CrossEntropy is commonly employed in classification problem as the ID loss. After the FC Layer and Softmax Layer, the output vector is probabilities for different classes which can be expressed as \mathbf{q} and the ground truth for this feature is \mathbf{p} which is a one-hot vector. Then the CrossEntropy can be formulated as:

$$\mathcal{H}(\mathbf{p}, \mathbf{q}) = - \sum_{i=1}^k p_i \log q_i \quad (7)$$

where k is the class number. Minimizing the CrossEntropy can make the predicted probabilities close to the ground truth.

In our training strategy, for a single mini-batch, there are different IDs with several bounding box images for each ID. So Triplet Loss and center loss are designed to guide the training process with feature distance. For Triplet Loss $\mathcal{L}_{Triplet}$ in this equation, we use hard Triplet Loss:

$$\mathcal{L}_{Triplet} = \sum_{i=1}^N \left[\alpha + \|\mathbf{f}_i^a - \mathbf{f}_i^p\|_2^2 - \|\mathbf{f}_i^a - \mathbf{f}_i^n\|_2^2 \right]_+ \quad (8)$$

where \mathbf{f}_i^a , \mathbf{f}_i^p , \mathbf{f}_i^n are the anchor feature, positive feature and negative feature, respectively. In order to improve performance after introducing Triplet Loss, we use the batch hard positive and negative features, which means:

$$\begin{cases} \mathbf{f}_i^p = \arg \max_{f_i^p} \|\mathbf{f}_i^a - \mathbf{f}_i^p\|_2^2 \\ \mathbf{f}_i^n = \arg \min_{f_i^n} \|\mathbf{f}_i^a - \mathbf{f}_i^n\|_2^2 \end{cases} \quad (9)$$

Center loss \mathcal{L}_C is designed to make samples with identical ID close to clustering center of this ID, which is formulated as:

$$\mathcal{L}_C = \frac{1}{2} \sum_{i=1}^m \|\mathbf{x}_i - \mathbf{c}_{y_i}\| \quad (10)$$

where \mathbf{c}_{y_i} denotes the feature center for the class of y_i .

Shown in the Figure 2, features from different branches are fed into different losses. Since Triplet Loss and center loss both are able to improve the clustering attribute of the output features, we name these losses as clustering loss. The global features and concatenated local features from all branches are guided by clustering loss. At the same time,

each local feature and global feature are separately passed into ID loss.

After feature extraction and before the FC layer, a feature normalization layer is used to constrain the features located at a hyper-sphere in feature space. During evaluation stage, instead of using Euclidean distance, we utilize the Cosine distance to measure the feature similarity and the experimental results prove that Cosine distance is more effective when describe the difference between features vectors. The Cosine distance can be denoted as:

$$similarity(X, Y) = \cos\theta = \frac{\mathbf{x} \cdot \mathbf{y}}{\|\mathbf{x}\| \cdot \|\mathbf{y}\|} \quad (11)$$

where \mathbf{x} and \mathbf{y} are two feature vectors between which the similarity need to be measured.

4. Experiments

In this section, we report the experimental results on our proposed Collaborative Attention Network. All the experiments are mainly conducted on the dataset of Market-1501 [31] which is the most widely-used image-based person ReID dataset. Besides Market-1501, in order to verify the robustness of our model, some other mainstream public ReID datasets are used which are DukeMTMC-ReID [12] and CUHK03 [21]. We firstly introduce these public datasets and the benchmarks to measure the model accuracy.

4.1. Datasets and Benchmarks

Market-1501 This dataset was built in the summer of 2015 and released by Zheng et al. and it is the most popular and high-quality image-based person ReID dataset. This dataset was captured by six cameras (five high-resolution cameras and one low-resolution camera) on campus of Tsinghua University. The dataset was separated into training set and testing set which is furtherly split into gallery and query for testing set. There are 1,501 person IDs and 12,936 bounding box images in total, in which one certain person was captured by at least two cameras. Bounding boxes in the query set are manually labeled while in the gallery set were labeled by DPM detector.

DukeMTMC-ReID This is a subset of DukeMTMC dataset and specifically for the person ReID task. There are 16,522 training images from 702 person IDs, 2,228 query images from another 702 person IDs and 17,661 gallery images from the same person IDs as query set. Images are sampled from video tracks by every 120 frames and all the videos are captured by eight high-resolution cameras on Duke campus. To maintain the high quality of bounding boxes, this dataset was labeled by hand instead of using pedestrian detectors.

CUHK03 This dataset is stored as MAT format file. There are 1,467 different person IDs in this dataset collected

by 5 pairs of cameras. The total 13,164 images are varied in image size and are separated into three groups: manually-labeled images for training, DPM-detected images for training and testing set. Along with the dataset, the paper mentioned two types of testing protocols. In order to keep the consistency of conclusions on different datasets, we chose the testing method where testing set is split into query and gallery.

Benchmarks The Cumulative Matching Characteristics (CMC) and mean average precision (mAP) are two commonly-used measurements of ReID model accuracy. For single-gallery-shot condition, we use the CMC top-k accuracy. In this algorithm, the feature distances between gallery samples and one certain query sample are sorted from small to large. The top-k accuracy equals to 1 if top-k ranked gallery samples contain query identity and equals to 0 otherwise. For multi-gallery-shot condition, such top-k accuracy cannot properly describe the model accuracy. Then mean average precision (mAP) is used to compute the mean of the precision for every query sample and it is suitable to measure the multi-gallery-shot circumstance. Generally, we use CMC top-1, top-3, top-5, top-10 and mAP as the benchmarks to measure performance of different methods.

4.2. Comparison of the Number of Sliced Parts

For our part-based method, we uniformly partition the feature maps into different number of slices. We argue that such slicing operation can theoretically help with obtaining local features much more detailed and discriminative which are beneficial for person ReID tasks. If too many parts are obtained from global feature maps, however in contrast, such over-detailed local features cannot retain representative attributes, which would conversely deteriorate the model performance. The following experiments are comparing the model performance when changing the number of how many parts local features are sliced into and the results are shown in Table 2.

patterns of how to partition	mAP	rank-1	rank-3	rank-5
part-1, 2, 3	86.6	94.4	97.2	97.9
part-1, 2, 3, 4	86.4	94.4	97.2	98.0
part-1, 3, 5	86.1	94.6	97.5	98.1
part-1, 3, 5, 7	85.4	94.3	97.2	98.0
part-1, 3, 5, 7, 9	83.9	93.9	96.9	97.9

Table 2. Comparison between different levels of how to partition global features into local features.

From Table 2, it can be seen that *part-1, 2, 3* which means the global features are evenly divided into 2 and 3 parts can achieve the highest accuracy with mAP equals to 86.6% and rank-1 equals to 94.4%. For the experiment of partial features the accuracy is that mAP equals to 86.6%

and rank-1 equals to 94.4% which is no higher than *part-1, 2, 3*. Since the *part-4* partial features are included in *part-2* partial features, it cannot bring in improvement if features are separated into multiple even numbers of parts. So in the following experiments in this Table, we divide feature maps into 3, 5, 7 and 9 parts and add branches of different partition levels step by step. It is clear that when gradually adding feature branches, the accuracy of models is descending and for *part-1, 3, 5, 7, 9* the accuracy is 83.9% for mAP and 93.9% for rank-1. We can conclude from the experimental results that simply increasing partial granularities cannot contribute to the improvement of models. In the next section, the effectiveness of our proposed method is proven by experimental results.

4.3. Effectiveness of Collaborative Attention

The Collaborative Attention (CA) mechanism is the key part in our proposed method. Improved from part-based methods, we concatenate neighbouring local features as collaborative local features in our network. We argue that our method can take advantage of subtle detail features and we could obtain more discriminative feature representations by combining partial features together. The results of methods with our proposed Collaborative Attention mechanism are shown in Table 3

Method	mAP	rank-1	rank-3	rank-5	rank-10
part-1,2,3 with CA	87.4	94.8	97.6	98.4	99.1
part-1,2,3,4 with CA	86.7	94.5	97.5	98.3	99.1
part-1,3,5 with CA	87.6	95.0	97.8	98.4	99.2
part-1,3,5,7 with CA	87.9	95.2	97.5	98.3	99.2
part-1,3,5,7,9 with CA	87.2	94.8	97.4	98.2	98.9
part-1,3,5,7 w/o CA	85.4	94.3	97.2	98.0	98.8
part-1,3,5,7 with CA	87.9	95.2	97.5	98.3	99.2

Table 3. Comparative experiments of part-based methods without/with Collaborative Attention mechanism.

Comparing Table 2 and Table 3, the difference between conducted experiments is that Collaborative Attention mechanism is adopted after features are partitioned. From each partitioning pattern experimental results, we conclude that our proposed CA mechanism can bring in improvement. In all combinations of how to separate features, *part-1, 3, 5, 7* achieves the best performance in which the CA mechanism raises model accuracy from mAP 85.4% and rank-1 94.3% to mAP 87.9% and rank-1 95.2%. In Table 2, part-based methods with higher level of partitioning show no advantage. After introducing the CA mechanism, more detailed partial features can have positive effects on producing more discriminate feature representations. Since we concatenate two adjacent image stripes in our CA mechanism, the partial feature will still lose conspicuousness if the global features are split into too many parts. As a result, the performance of *part-1, 3, 5, 7, 9* is no better than

part-1, 3, 5, 7.

4.4. Combination of Loss Functions

Multi-loss functions are used in our proposed method, in which we combine ID loss with Triplet Loss and Center Loss. ID Loss is to improve the classification abilities for the model while Triplet Loss and Center Loss can make output features more discriminative. In the experiments, we compare the results when we progressively introduce CrossEntropy \mathcal{L}_{CE} , triplet Loss \mathcal{L}_{trip} and Center Loss \mathcal{L}_C . We also argue that it would be useful if the outputs from both global and local branches are guided by Triplet Loss and Center Loss, unlike the loss function strategy in MGN [20] in which only global features play a part in Triplet Loss. The results for loss-function-related experiments are shown in Table 4

Loss Combination	mAP	rank-1	rank-3	rank-5
CAN+ \mathcal{L}_{CE}	87.0	95.0	97.8	98.7
CAN+ \mathcal{L}_{CE} + \mathcal{L}_{Trip}	87.9	95.2	97.5	98.3
CAN+ \mathcal{L}_{CE} + \mathcal{L}_{Trip} + \mathcal{L}_C	88.3	95.4	97.6	98.4
global & local to \mathcal{L}_C	89.6	95.7	97.8	98.6

Table 4. Experimental results of progressively adding different loss functions and comparative results between solely global features and twofold (global and local) features in clustering loss function $\mathcal{L}_c = \mathcal{L}_{Trip} + \mathcal{L}_C$.

If only ID Loss (CrossEntropy) is employed as loss function, our proposed Collaborative Attention Network (CAN) can achieve the performance mAP/rank-1=87.0%/95.0%. Triplet Loss and Center Loss can enhance features clustering attributes and we name these two loss functions as clustering loss. We firstly take global features into calculation of clustering loss as what the existing methods do. After combining Triplet Loss with ID Loss (CrossEntropy), CAN achieves mAP/rank-1=87.9%/95.2% and when Center Loss is adopted, the accuracy is improved to mAP/rank-1=88.3%/95.4%. Then we furtherly use features from local branches as input of clustering loss to guide the training process, the model achieves the best performance with mAP 89.6% and rank-1 95.7%. So supervising each local feature by loss functions during training process can enhance the feature performance when testing.

4.5. Implement Details

In this section, we introduce the details of how we set up the training strategy for the Collaborative Attention Network. Since we apply Triplet Loss and Center Loss in our loss function, we set the mini-batch to 32 images in which 8 different person IDs are randomly picked with 4 bounding boxes images for each ID. All input bounding boxes are resized to 384×128 with height

of 384 and width of 128. The loss function is a multi-loss function with CrossEntropy, Triplet Loss and Center Loss and the weight of Center Loss in this function is set to 0.0005. Adam optimizer is utilized with default parameters ($\epsilon = 10^{-8}$, $\beta_1 = 0.9$, $\beta_2 = 0.999$). The initial learning rate is 3×10^{-4} and the learning rate is decayed to 3×10^{-5} at epoch 250, decayed to 3×10^{-6} at epoch 350 and decayed to 3×10^{-7} at epoch 450. The whole training process stops at epoch 600. Since we normalize the features and weights in FC Layer, we use the cosine distance as metrics to measure feature similarity during testing process.

Feature&metric	mAP	rank-1	rank-3	rank-5
w/o normalize + euclidean	89.6	95.7	97.8	98.6
w/o normalize + cosine	89.7	95.8	98.0	98.6
with normalize + euclidean	90.1	95.8	98.1	98.7
with normalize + cosine	90.6	96.4	98.3	98.8

Table 5. Comparative experiments on whether features are normalized before FC Layer and the distance metrics at the validation stage.

From Table 5, if we use the final FC Layer without normalization, the model accuracy is mAP/rank-1=89.6%/95.7% and 89.7%/95.8% respectively for using euclidean distance and cosine distance as feature distance. In the situation, different measurements do not bring in remarkable changes on model accuracy. After normalizing features and weights in FC Layer, if euclidean distance is used during testing, the performance is mAP 90.1% and rank-1 95.8%. Then cosine distance is used as measurement of the model with normalization, the accuracy is mAP 90.6% and rank-1 96.4% which is the best performance among all our experiments.

4.6. Comparison with the State-of-the-art Methods

In this section, we compare the results on our proposed method with existing state-of-the-art image-based person ReID methods on the dataset of Market-1501. In order to show the generality and robustness of our model, we conduct experiments on datasets of DukeMTMC-ReID and CUHK03 as extended datasets. In some works, re-ranking method were used to improve mAP and rank-1 accuracy. However, we argue that the actual performance of models cannot be revealed after re-ranking So our experimental results are based on model accuracy without re-ranking. Table 6 shows the comparison with existing image-based person ReID on Market-1501 and Table 7 shows the comparison results on DukeMTMC-ReID and CUHK03 datasets.

In Table 6, the existing state-of-the-art method is a pyramidal approach proposed in [30] whose accuracy is mAP/rank-1=88.2%/95.7%, but our proposed method achieves mAP/rank-1=90.6%/96.4% which exceeding the previous best performance by 2.4% in mAP and 0.7% in rank-1.

In Table 7, the pyramidal method still achieved the best performance among all previous approaches with mAP 82.3% and rank-1 91.6% on DukeMTMC-ReID. In CUHK03 datasets, bounding box images are both artificially labeled and detected by detectors. Some of the previous works were tested on labeled and detected images respectively and we select the better performance in this table. In our experimental settings for CUHK03, all testing images are used without splitting into labeled and detected groups. As what is shown in this table, our method achieves mAP 82.8% and rank-1 86.1% in model accuracy, which also outperforms all published methods by a large margin. Our proposed Collaborative Attention Network achieves state-of-the-art performance which indicates the robustness of our method.

Method	mAP	rank-1	rank-5	rank-10
Spindle [28]	-	76.9	91.5	94.6
SVDNet [18]	62.1	82.3	92.3	95.2
PDC [17]	63.4	84.1	92.7	94.9
PSE [14]	69.0	87.7	94.5	96.8
Cam-style [33]	71.6	89.5	-	-
GLAD [23]	73.9	89.9	-	-
HA-CNN [10]	75.7	91.2	-	-
CNN-Base [3]	79.8	92.5	-	-
PCB+RPP [19]	81.6	93.8	97.5	98.5
HPM [4]	82.7	94.2	97.5	98.5
SGGNN [16]	82.8	92.3	96.1	97.4
SPReID [9]	83.4	93.7	97.6	98.4
MHN [1]	85.0	95.1	98.1	98.9
DG-Net [32]	86.0	94.8	-	-
MGN [20]	86.9	95.7	-	-
DSA-ReID [27]	87.6	95.7	-	-
Pyramid [30]	88.2	95.7	98.4	99.0
CAN(ours)	90.6	96.4	98.8	99.3

Table 6. Comparing with current state-of-the-art methods on Market-1501.

5. Conclusion

In this paper, we novelly propose the multi-branch Collaborative Attention Network (CAN), a feature extractor for person ReID task. We find out the best combination of numbers of parts sliced from global feature maps and conclude that partition global features into too many will conversely reduce the model accuracy. Unlike other existing part-based methods, we concatenate local features by collaborative attention mechanism to form more effective feature representations. Our modification on loss functions in which both global and local branches are imported into Triplet Loss and Center Loss. Through comparative experiments, we address

Method	DukeMTMC-ReID		CUHK03	
	mAP	rank-1	mAP	rank-1
CNN-Base [3]	68.5	83.5	59.0	63.5
PSE+ECN [14]	62.0	79.8	30.2	27.3
Cam-style [33]	57.6	78.3	-	-
GLAD [23]	-	-	-	85.0
HA-CNN [10]	63.8	80.5	41.0	44.4
PCB+RPP [19]	69.2	83.3	57.5	63.7
HPM [4]	74.3	86.6	63.9	57.2
MHN [1]	77.2	89.1	65.4	77.2
DG-Net [32]	74.8	86.6	-	-
MGN [20]	78.4	88.7	67.4	68.0
DSA-ReID [27]	74.3	86.2	75.2	78.9
Pyramid [30]	79.0	89.0	76.9	78.9
CAN(ours)	82.3	91.6	82.8	86.1

Table 7. The comparison with existing image-based Re-ID approaches on DukeMTMC-ReID and CUHK03.

that our proposed approach outperforms the existing state-of-the-art methods on the public datasets.

References

- [1] Binghui Chen, Weihong Deng, and Jiani Hu. Mixed high-order attention network for person re-identification.
- [2] Jia Deng, Wei Dong, Richard Socher, Li-Jia Li, and Fei-Fei Li. Imagenet: a large-scale hierarchical image database. In *2009 IEEE Computer Society Conference on Computer Vision and Pattern Recognition (CVPR 2009)*, 20-25 June 2009, Miami, Florida, USA, 2009.
- [3] Xiong Fu, Xiao Yang, Zhiguo Cao, Kaicheng Gong, and Joey Tianyi Zhou. Towards good practices on building effective cnn baseline model for person re-identification. 2018.
- [4] Yang Fu, Yunchao Wei, Yuqian Zhou, Honghui Shi, Gao Huang, Xinchao Wang, Zhiqiang Yao, and Thomas Huang. Horizontal pyramid matching for person re-identification.
- [5] Kaiming He, Xiangyu Zhang, Shaoqing Ren, and Jian Sun. Deep residual learning for image recognition. In *Proceedings of the IEEE conference on computer vision and pattern recognition*, pages 770–778, 2016.
- [6] Alexander Hermans, Lucas Beyer, and Bastian Leibe. In defense of the triplet loss for person re-identification. 2017.
- [7] Jie Hu, Li Shen, Samuel Albanie, Gang Sun, and Enhua Wu. Squeeze-and-excitation networks.
- [8] Eldar Insafutdinov, Leonid Pishchulin, Bjoern Andres, Mykhaylo Andriluka, and Bernt Schiele. Deepcut: A deeper, stronger, and faster multi-person pose estimation model. 2016.
- [9] Mahdi M. Kalayeh, Emrah Basaran, Muhittin Gokmen, Mustafa E. Kamasak, and Mubarak Shah. Human semantic parsing for person re-identification. In *2018 IEEE/CVF Conference on Computer Vision and Pattern Recognition (CVPR)*, 2018.
- [10] Wei Li, Xiatian Zhu, and Shaogang Gong. Harmonious attention network for person re-identification.
- [11] Hao Luo, Youzhi Gu, Xingyu Liao, Shenqi Lai, and Wei Jiang. Bags of tricks and a strong baseline for deep person re-identification. 2019.
- [12] Ergys Ristani, Francesco Solera, Roger Zou, Rita Cucchiara, and Carlo Tomasi. Performance measures and a data set for multi-target, multi-camera tracking. In *European Conference on Computer Vision workshop on Benchmarking Multi-Target Tracking*, 2016.
- [13] Zhao Rui, Wanli Ouyang, and Xiaogang Wang. Learning mid-level filters for person re-identification. 2014.
- [14] M. Saquib Sarfraz, Arne Schumann, Andreas Eberle, and Rainer Stiefelwagen. A pose-sensitive embedding for person re-identification with expanded cross neighborhood re-ranking. In *CVPR 2018*, 2017.
- [15] Evan Shelhamer, Jonathan Long, and Trevor Darrell. *Fully Convolutional Networks for Semantic Segmentation*. 2017.
- [16] Yantao Shen, Hongsheng Li, Shuai Yi, Dapeng Chen, and Xiaogang Wang. Person re-identification with deep similarity-guided graph neural network.
- [17] Chi Su, Jianing Li, Shiliang Zhang, Junliang Xing, Wen Gao, and Qi Tian. Pose-driven deep convolutional model for person re-identification.
- [18] Yifan Sun, Zheng Liang, Weijian Deng, and Shengjin Wang. Svdnet for pedestrian retrieval. 2017.
- [19] Yifan Sun, Zheng Liang, Yang Yi, Tian Qi, and Shengjin Wang. Beyond part models: Person retrieval with refined part pooling (and a strong convolutional baseline). 2017.
- [20] Guanshuo Wang, Yufeng Yuan, Chen Xiong, Jiwei Li, and Zhou Xi. Learning discriminative features with multiple granularities for person re-identification. 2018.
- [21] Li Wei, Zhao Rui, Xiao Tong, and X. G. Wang. Deepreid: Deep filter pairing neural network for person re-identification. 2014.
- [22] Longhui Wei, Shiliang Zhang, Gao Wen, and Tian Qi. Person transfer gan to bridge domain gap for person re-identification. 2018.
- [23] Longhui Wei, Shiliang Zhang, Hantao Yao, Wen Gao, and Qi Tian. Glad: Global-local-alignment descriptor for pedestrian retrieval.
- [24] Yandong Wen, Kaipeng Zhang, Zhifeng Li, and Qiao Yu. *A Discriminative Feature Learning Approach for Deep Face Recognition*. 2016.
- [25] Fan Xing, Jiang Wei, Luo Hao, and Mengjuan Fei. Spherereid: Deep hypersphere manifold embedding for person re-identification. 2018.
- [26] Hantao Yao, Shiliang Zhang, Yongdong Zhang, Jintao Li, and Tian Qi. Deep representation learning with part loss for person re-identification. 28(6):2860–2871, 2019.
- [27] Zhizheng Zhang, Cuiling Lan, Wenjun Zeng, and Zhibo Chen. Densely semantically aligned person re-identification.
- [28] Haiyu Zhao, Maoqing Tian, Shuyang Sun, Shao Jing, and Xiaoou Tang. Spindle net: Person re-identification with human body region guided feature decomposition and fusion. In *2017 IEEE Conference on Computer Vision and Pattern Recognition (CVPR)*, 2017.
- [29] Liming Zhao, Xi Li, Yueting Zhuang, and Jingdong Wang. Deeply-learned part-aligned representations for person re-identification. 2017.
- [30] Feng Zheng, Cheng Deng, Xing Sun, Xinyang Jiang, Xiaowei Guo, Zongqiao Yu, Feiyue Huang, and Rongrong Ji. Pyramidal person re-identification via multi-loss dynamic training.
- [31] Liang Zheng, Liyue Shen, Lu Tian, Shengjin Wang, Jingdong Wang, and Qi Tian. Scalable person re-identification: A benchmark. pages 1116–1124, 12 2015.
- [32] Zhedong Zheng, Xiaodong Yang, Zhiding Yu, Liang Zheng, Yi Yang, and Jan Kautz. Joint discriminative and generative learning for person re-identification.
- [33] Zhun Zhong, Liang Zheng, Zhedong Zheng, Shaozi Li, and Yi Yang. Camera style adaptation for person re-identification. 2017.